

*Transport and Telecommunication, 2010, Volume 11, No 4, 14–28*  
*Transport and Telecommunication Institute, Lomonosova 1, Riga, LV-1019, Latvia*

## APPROACH TO HARDWARE IMPLEMENTATION OF GENETIC ALGORITHM FOR INVERSE PROBLEM OF ROADWAY COVERAGE SUBSURFACE PROBING SOLUTION

**A. Krainyukov, V. Kutev, D. Opolchenov**

*Transport and Telecommunications Institute  
 Lomonosova str. 1, Riga, LV-1019, Latvia  
 Ph.: +371 67100634. Fax: +371 67100660*

*E-mail: Aleksandrs.Krainukovs@tsi.lv, Valerijs.Kutev@tsi.lv, Daniil.Opolchenov@tsi.lv*

This work has focused on the problem of approach to hardware implementation of genetic algorithm for inverse problem of roadway coverage subsurface radar probing solution. Iterative procedure to solve the inverse problem in frequency domain is used on base of aim function minimization. Genetic algorithm is used for search of global minimum of aim function. For hardware implementation of genetic algorithm it is necessary correctly to choose the values of arguments for aim function and parameters of genetic algorithm. The authors investigated two different kinds of aim functions. Estimation of possibility for genetic algorithm hardware implementation on base of field-programmable gate array (FPGA) is discussed.

**Keywords:** roadway radar monitoring, inverse problem, genetic algorithm, field-programmable devices, hardware implementation

### 1. Introduction

Roadway structure is a complex multi-layered construction, various layers of which consist of materials of different durability. It is well-known that in different times of the year and in different environmental conditions the preservation of road cover depends not only on its usage but also on different climate-related factors.

For optimisation of exploitation, upkeep and reconstruction of road cover certain information is crucial, such as condition of its internal layers and the processes taking place within them: the appearance of potholes, changes in dampness of the soil, changes in the ability of the soil to filter water, etc. Timely identification of these processes allows one to make an informed decision about the necessary actions. This is why it is necessary to constantly monitor the condition of the inner layers of the road structure, in order to act in time in response to the changes the state of its layers.

In present time to research the inner structure of objects, of both artificial and natural origin, subsurface radar probing methods are widely used [1, 2]. The latter allows one to ascertain the thickness of the inner layers of the road structure, the degree and quality of compactness of various road components, as well as to identify areas of excessive dampness, potholes and sources of water penetration. Determining pavement thickness, detected voids beneath pavement and measuring the moisture content in pavement layers are examples of such using. However, traditional methods of interpretation of the results of the subsurface radar probing of roadways do not provide the required precision and effectiveness of the road monitoring. Transportation departments need better methods for measuring near-surface and subsurface conditions of their transportation facilities [2]. It is possible to increase the precision of diagnosis and identification of inner zones and objects based on the results of radar subsurface probing through reconstruction of the geometrical and electro-physical characteristics, which leads to the necessity to solve the inverse problem of radar subsurface probing. Reconstruction of electro-physical characteristics of the road structure is in essence identification of electro-physical parameters of the layers of the road structure, which can be achieved by solving the inverse structure problem of subsurface radar probing.

In [3,4] we will look at the specifics of solving the inverse structure problem of subsurface radar probing in the frequency domain with through using a generic algorithm for search of global minimum of aim function.. Block diagram of iterative procedure to solve radar inverse problem is shown on Figure 1.

The initial stage of the iterative procedure is concerned with calculating of module spectral density  $|\dot{S}_e(\omega, \vec{P})|$  for reflected signal  $U_{ref}(t)$ . Further, in order to solve the inverse problem of subsurface radar probing, we introduce vector of parameters:

$$\vec{P} = \{p_1, p_2, \dots, p_n\} \in \vec{P}_{POS}, \quad (1)$$

where  $\vec{P}_{POS}$  – is a set of possible (allowed) values for parameters of probed area. The set of allowed values for parameters is determined on the basis of pre-existing hypotheses about internal structure of probed medium.

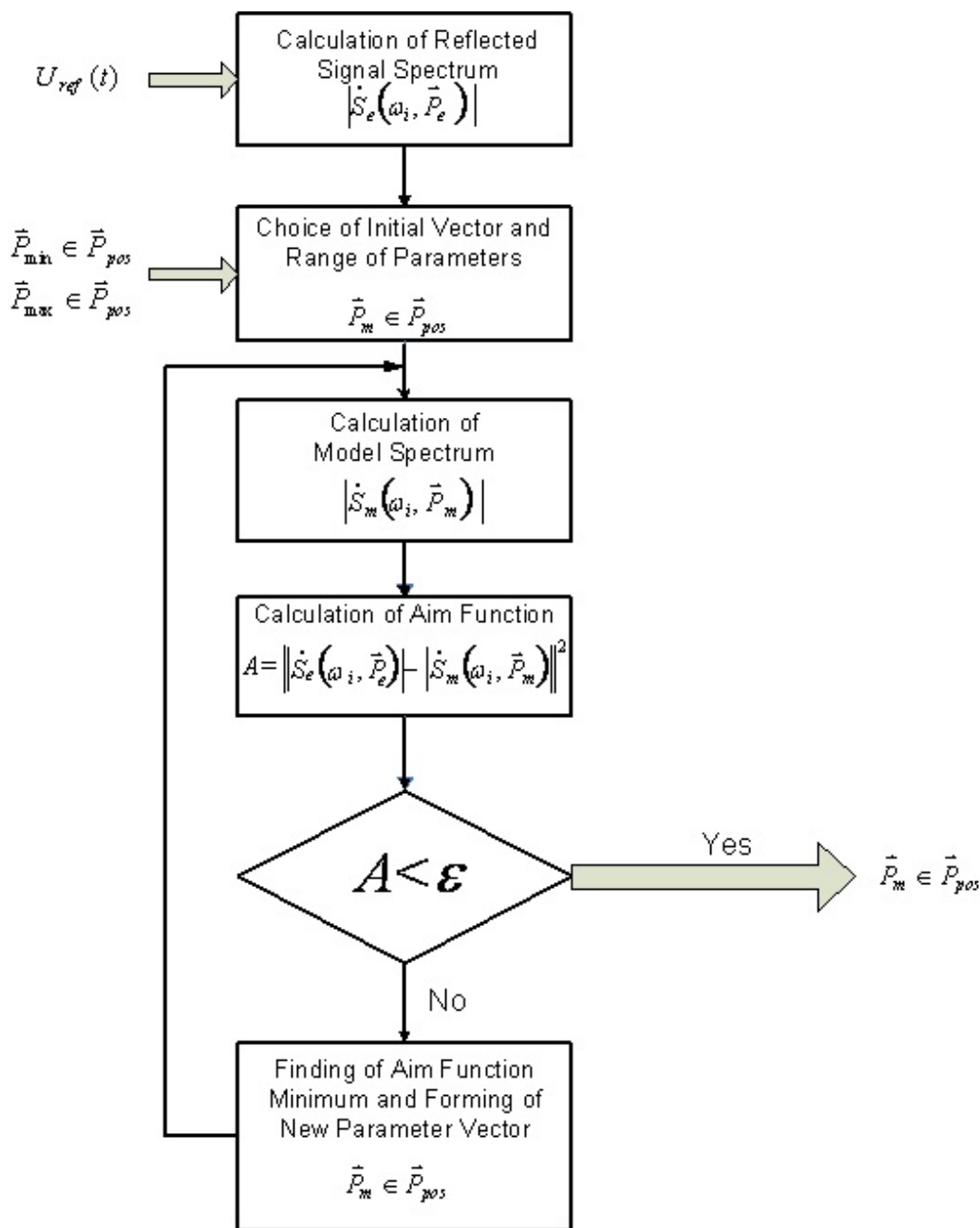


Figure 1. Block diagram of iterative procedure to solve radar inverse problem in frequency domain

Calculating of theoretical spectral density  $\dot{S}_T(\omega_i, \vec{P})$  equates to the solving of the direct problem of subsurface radar probing. To calculate  $\dot{S}_T(\omega_i, \vec{P})$  we chose the starting vector of parameters  $\vec{P}_M$  belonging to the set of allowed values of parameters  $\vec{P}_{POS}$ .

The choice of the starting vector of parameters is also determined on the basis of pre-existing hypotheses about the object of probing.

Values of the modules of experimental and theoretical spectral densities are used to calculate aim function  $\Phi_1$ :

$$\Phi_1 = \left\| \dot{S}_e(\omega_i, \bar{P}) - \dot{S}_T(\omega_i, \bar{P}_M) \right\|^2 = \frac{1}{n_{\max}} \sum_{i=0}^{n_{\max}} \left\| \dot{S}_e(\omega_i, \bar{P}) - \dot{S}_T(\omega_i, \bar{P}_M^j) \right\|^2, \quad (2)$$

where  $n_{\max}$  – index of the spectral component with frequency  $f_{\max}$ .

If the value of the aim function  $\Phi_1$  is not more than the value of a threshold  $\alpha$ , then solving the inverse structure problem is finished. The solution (pseudo-solution) is the vector of parameters  $\bar{P}_M$ . If the value of the aim function  $\Phi_1$  is greater than the value of  $\alpha$ , then taking into account the current values of the vector  $\bar{P}_M$  we formulate a new vector of parameters  $\bar{P}_M^j$ , which is used to calculate new values of the aim function  $\Phi_1$ . This means, that finding a solution to the inverse problem in the form of the vector  $\bar{P}_M$  is performed by iteration with the sequential improvement of accuracy of the parameters  $\bar{P}_M$ .

It has been suggested [4] that the value of  $\alpha$  is set as follows:

$$\alpha = \frac{P_{av}}{K}, \quad (3)$$

where  $P_{av}$  – the averaged mean power of those spectral components  $\dot{S}_e(\omega_i, \bar{P})$ , which are used for calculating of aim function  $\Phi_1$ , and  $K$  – dimensionless coefficient, set by the user.

In [3,4] we researched the effect of the conditions of solving the inverse problem and parameters of generic algorithm on the error of restoration of electro-physical parameters of the modelled three-layered medium. The value of the electro-physical parameters of the layers of the two-layered medium being modelled (layer thickness  $h$ , electrical conductivity  $\sigma$  and the relative dielectric permittivity  $\varepsilon$ ) corresponded to the electro-physical parameters of the materials of the layers road structure. It was determined that the error of restoration of electro-physical parameters can reach up to 10% and the results of restoration depends significantly on the assumptions about the parameters of the modelled two-layered medium. Optimal values of the coefficient  $K$  from the point of view of restoration of the parameters of the road surface and iteration of the algorithm lie within range from 1000 to 3000.

When solving the inverse problem of sub-layer probing it is very important to rationally select the original inputs, which are determined by various informational characteristics, scope of their existence and their quantities.

In aim function (2), used in [3, 4], informational characteristic used was the spectral density of the reflected signal is in the form of its modular values ( $|\dot{S}_e(\omega_i, \bar{P})|$  and  $|\dot{S}_T(\omega_i, \bar{P}_M)|$ ). However, this informational characteristic can also be used in the form of complex values. In this case the expression for calculation of aim function  $\Phi_2$  is as follows:

$$\Phi_2 = \left\| \dot{S}_e(\omega_i, \bar{P}) - \dot{S}_T(\omega_i, \bar{P}_M) \right\|^2 = \frac{1}{n_{\max}} \sum_{i=0}^{n_{\max}} \left| \dot{S}_e(\omega_i, \bar{P}) - \dot{S}_T(\omega_i, \bar{P}_M^j) \right|^2, \quad (4)$$

and the algorithm of solving the inverse structural problem of subsurface probing stays the same (Fig. 1).

Irrespective of the form of the informational characteristic aim functions  $\Phi_1$  and  $\Phi_2$  greatly depend on the parameters of the probing medium and frequency range, in which the inverse structure problem of subsurface probing is being solved. Apart from the global minimum aim functions  $\Phi_1$  and  $\Phi_2$  have numerous false local minimums, which give possible incorrect solutions to the inverse problem.

In this work we research the effect of electro-physical parameters of the three-layer modelled medium on the behaviour of aim functions  $\Phi_1$  and  $\Phi_2$ . For the chosen model of the probed medium, probing signal and aim functions  $\Phi_1$  and  $\Phi_2$ , we solve the inverse problem using, according to the block diagram of iterative procedure shown on Figure 1, we research the effect of GA characteristics on the time for solving the of inverse problem, we research the hardware implementation of genetic algorithm on FPGA.

## 2. Analysis of Aim Functions for the Inverse Problem of Roadway Coverage Radar Subsurface Probing

### 2.1. Models of the roadway coverage and of the probe signal

The model of roadway coverage may be conceived as homogeneous horizontal layers: first layer-pavement and second layer -base, which are placed between two semi-infinite spaces: upper-air and lower-sub grade. Used model of probe signal was the same as in [3].

Calculation of theoretical spectral density is performed by multiplying of the spectrum of the probe signal and the theoretical coefficient of reflection of the medium  $\dot{R}_T(\omega_i, \vec{P}_M)$  [3,4], which is described by the vector  $\vec{P}_M$ :

$$\dot{S}_T(\omega_i, \vec{P}) = \dot{S}(\omega_i) \cdot \dot{R}_T(\omega_i, \vec{P}_M). \quad (5)$$

### 2.2. Influence of electro-physical parameters of the medium on aim functions

Aim functions  $\Phi_1$  and  $\Phi_2$  of the inverse problem of radar subsurface probing being solved are functions of parameter vector  $\vec{P}$  and used frequency spectrum of reflected signal which has maximal frequency  $f_{max}$ . For the studied model of the probed medium the number of arguments of aim functions  $\Phi_1$  and  $\Phi_2$  equals 9, i.e. 8 electro physical parameters of the model medium [4] and maximal frequency  $f_{max}$ .

In order to demonstrate the dependency of the aim functions on electro physical parameters in three-dimensional form we selected two partial arguments for calculations of them.

To calculate the value of the theoretical spectral density  $\dot{S}_T(\omega_i, \vec{P})$  we were changing the values of two of the electro physical parameters of one of the layers of the medium while keeping the remaining 6 constant and equal to the modelled ones. The range of changes of the chosen parameters was symmetrical to the modelled values and equal to them.

#### 2.2.1. Dependence of aim functions on dielectric permittivity and thickness of the layers

Dependencies of aim functions  $\Phi_1$  and  $\Phi_2$  on dielectric permittivity  $\varepsilon'$  of the layers and their thickness  $h$  are shown on Figures 2 and 3.

In the upper part of each figure there is a three-dimensional view of the dependence of the aim function on two parameters calculated for  $f_{max} = 300$  MHz, and in the bottom part – the level of the functions depends on two parameters for three values of maximal frequency  $f_{max} = 100, 300$  and 500 MHz. For the minimal level the threshold value  $\alpha$  was used. In all of the diagrams for aim functions the value  $\alpha$  was used, calculated using  $K = 2000$ .

The areas of aim functions  $\Phi_1$  and  $\Phi_2$  with values less than  $\alpha$ , are shown in the centre of the diagrams and highlighted in white. The geometric form of these areas allows us to judge the degree of the effect of each parameter on the aim function.

The geometric forms of the white areas show on Figure 2 and Figure 3 are ellipses, but of different sizes. Comparative analysis of these areas allows us to make the following:

- dielectric permittivity and thickness of layers heavily affect the values of aim functions  $\Phi_1$  and  $\Phi_2$ ;
- calculation of the aim functions for  $f_{max} > 300$  MHz increases the size and compression of the ellipses, which means that in order to calculate aim functions it is crucial, that  $f_{max}$  is less than 300 MHz;
- aim function  $\Phi_2$  with a complex spectral density is more informative, because areas taking values less than  $\alpha$  are smaller in size, i.e. corresponding ranges of  $h_1$  and  $\varepsilon'_1$  on the diagrams for  $\Phi_2$  are less than those for  $\Phi_1$ ;
- values of aim functions  $\Phi_1$  and  $\Phi_2$  less than  $\alpha$ , are obtainable under multidirectional changes of dielectric permittivity and thickness of the layers against the modelled values of the parameters of the layers, which can lead to errors of reconstruction of parameters of the probed medium.

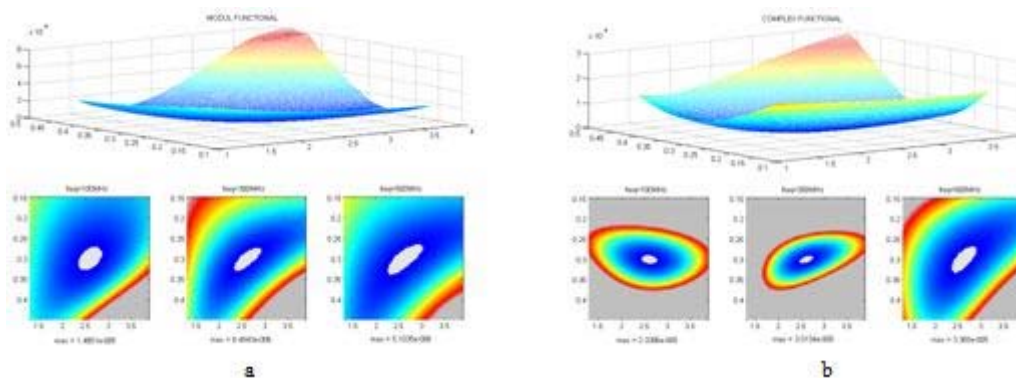


Figure 2. Influence of dielectric permittivity  $\epsilon_1'$  and thickness  $h_1$  of the first layer (pavement) on the aim functions  $\Phi_1(a)$  and  $\Phi_2(b)$

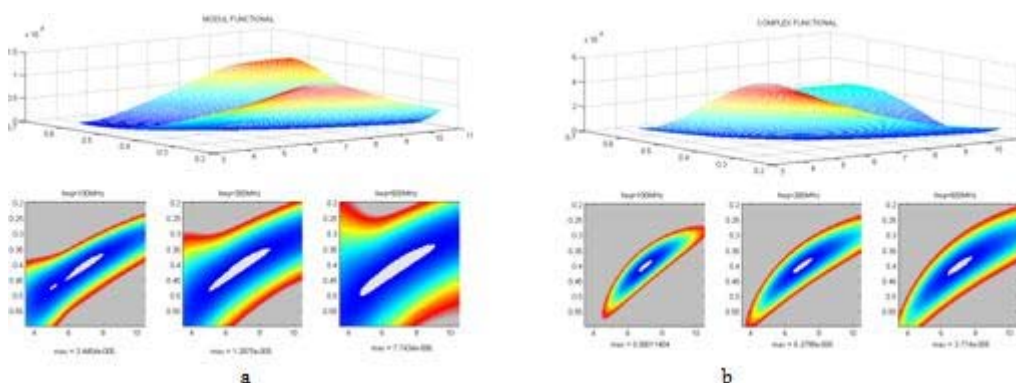


Figure 3. Influence of dielectric permittivity  $\epsilon_2'$  and thickness  $h_2$  of the second layer (base) on the aim functions  $\Phi_1(a)$  and  $\Phi_2(b)$

2.2.2. Dependencies of aim functions on the electrical conductivity of the layers

Dependencies of aim functions  $\Phi_1$  and  $\Phi_2$  on the electrical conductivity of the first layer  $\sigma$  and on two other parameters are shown in the Figure 4. Conditions of calculations, representations and values of  $f_{max}$  are the same as those shown in the Figure 2 and Figure 3.

The geometrical form of the white areas is close to a rectangle, the length of which is equal to the range of changes of electrical conductivity of the layer, and the width depends on the second electro-physical parameter of the layer or the width of the frequency range (value  $f_{max}$ ). This means that the influence of the electrical conductivity of the layers on the values of the aim functions is negligible. Electrical conductivity  $\sigma_2$  and  $\sigma_3$  affect aim functions similarly.

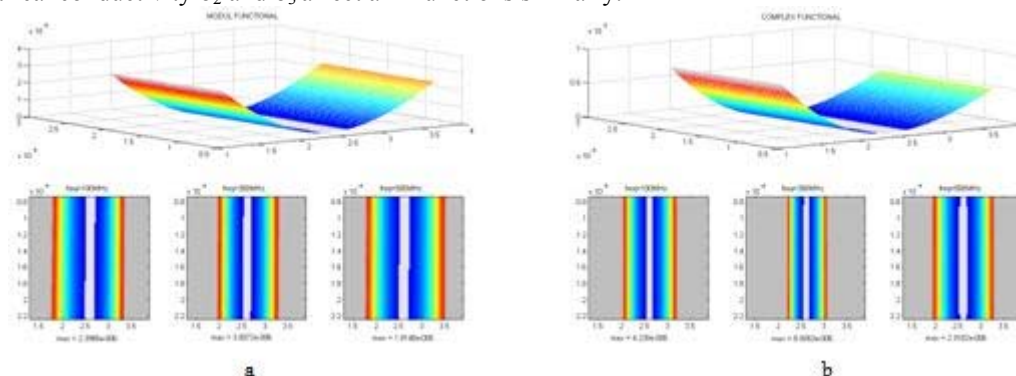


Figure 4. Influence of dielectric permittivity  $\epsilon_1'$  and electrical conductivity  $\sigma_1$  of the first layer (pavement) on the aim functions  $\Phi_1(a)$  and  $\Phi_2(b)$

2.2.3. Influence of the parameters of lower semi-infinite space (sub grade) on the aim functions

On Figure 5 we have shown the influence of dielectric permittivity  $\epsilon'_3$  and electrical conductivity  $\sigma_3$  of lower semi-infinite space (sub grade) on the aim functions  $\Phi_1$  and  $\Phi_2$ . The affect of these parameters is quite significant: the shape of the areas corresponding to the minimal values of the aim functions (less than  $\alpha$ ) is close to a circle and their sizes are minimal compared to the similar areas in previous figures. Therefore, the aim functions  $\Phi_1$  and  $\Phi_2$  are very sensitive to changes in  $\epsilon'_3$  and  $\sigma_3$ , particularly the function  $\Phi_2$ . The increase of  $f_{max}$  leads to increase of these areas, hence for the solution of the inverse problem it is crucial that  $f_{max}$  does not exceed 300 MHz

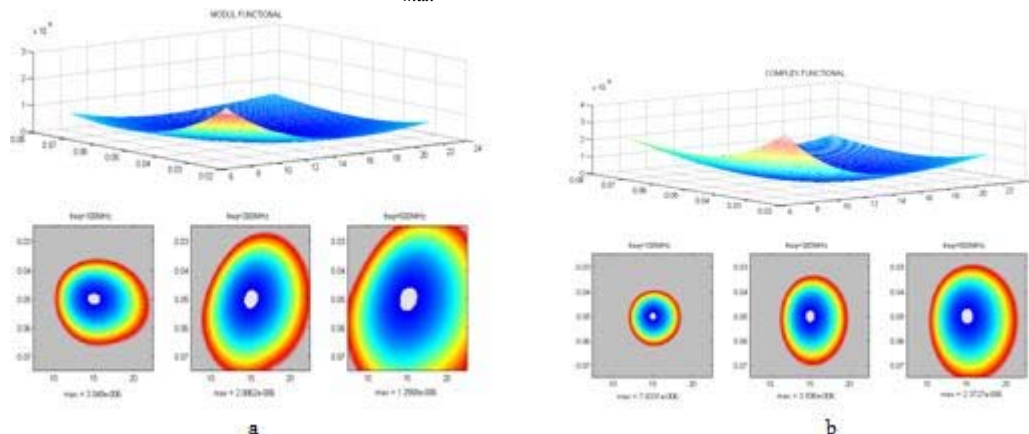


Figure 5. Influence of dielectric permittivity  $\epsilon'_3$  and electrical conductivity  $\sigma_3$  of lower semi-infinite space (sub grade) on the aim functions  $\Phi_1$  (a) and  $\Phi_2$  (b)

3. Results of Roadway Coverage Parameters Reconstruction with Using Aim Functions  $\Phi_1$  and  $\Phi_2$

For the chosen model of roadway coverage, probing signal and the aim functions  $\Phi_1$  and  $\Phi_2$  the solution of the inverse structural problem was carried out using generic algorithm (GA). In order to find the global minimal values generic algorithm was used with the same parameters as in [3-5].

The solution of the above problem – vector  $\vec{P}_M$  was used to access the relative error of reconstruction of each of the parameters of the modelled medium. At the same time the mean number of repetitions, necessary to finish the generic algorithm, was accessed.

In order to define the optimal conditions for the generic algorithm (GA) used to solve the inverse problem of radar `subsurface probing we researched how these values are influenced by the following factors:

- coefficient K, defining the threshold of the acceptable solution  $\alpha$ ;
- frequency range of used reflected signal spectrum, limited by its maximal frequency  $f_{max}$ .

To obtain statistical assessment about 100 solutions of the inverse problem for two layer model of roadway structure were used.

3.1. Influence of value coefficient  $\kappa$  on the errors of roadway model parameters reconstruction

The value of K in our calculations was changed within the range of 100 to 5000 with fixed  $f_{max} = 300$  MHz.

**Influence of value K on first layer (pavement) parameters reconstruction** On Figures 6 and 7 we show dependencies of the relative error (upper figures) and relative root-mean-square (SMR) error (lower figures) of the results of reconstruction of electro-physical parameters of the first layer (pavement) on value coefficient K.

When using the aim function  $\Phi_2$  the relative errors of reconstruction  $\epsilon_l$  and  $h_1$  are less than when using aim function  $\Phi_1$ , and are, in fact, close to 0 (this is clearly illustrated on Figure 2). When  $K \geq 1000$   $\epsilon_l$  and  $h_1$  slightly decrease.

Dependencies of relative RMS error for the first layer parameters show that the increase of  $K$  will result in a smaller range of possible values of  $\varepsilon_1$  and  $h_1$  (Figure 2).

Dependencies of relative RMS error for the first layer parameters show that the increase of  $K$  will result in a smaller range of possible values of  $\varepsilon_1$  and  $h_1$  (Figure 2). The range of possible values of  $\sigma_1$  remains unchanged with the increase of  $K$  (Figure 4); therefore the values of relative RMS error for  $\sigma_1$  are stable and significant. For this reason dependencies of  $\sigma_1$  have a chaotic character.

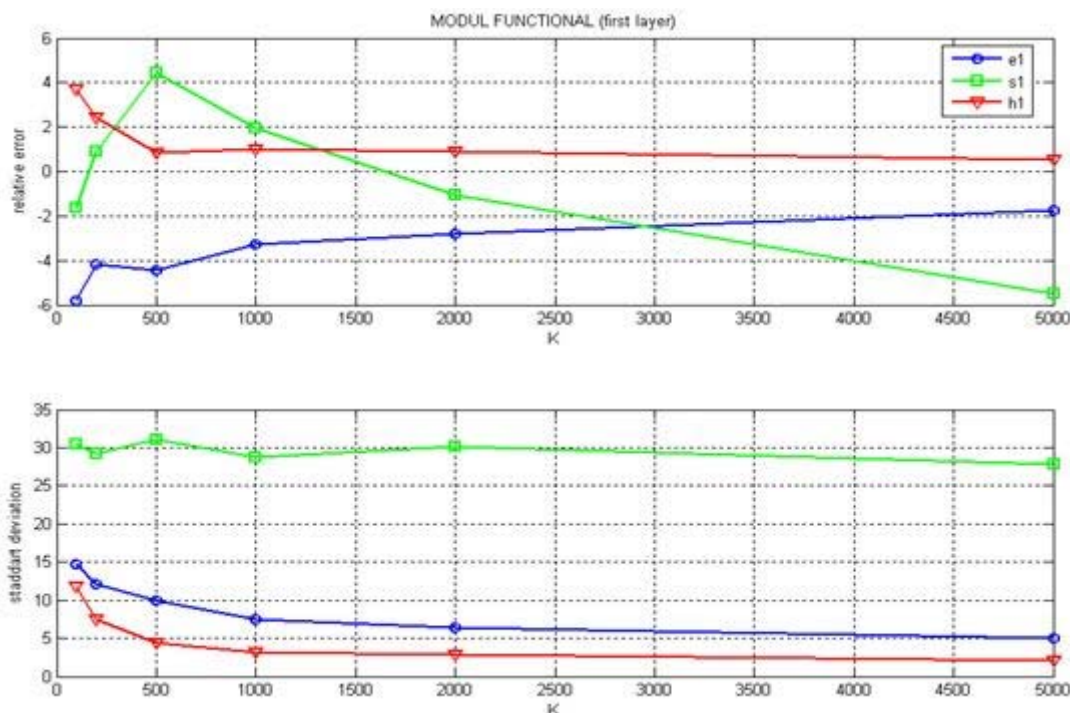


Figure 6. Influence of value  $K$  on accuracy reconstruction of first layer (pavement) parameters for using aim function  $\Phi_1$

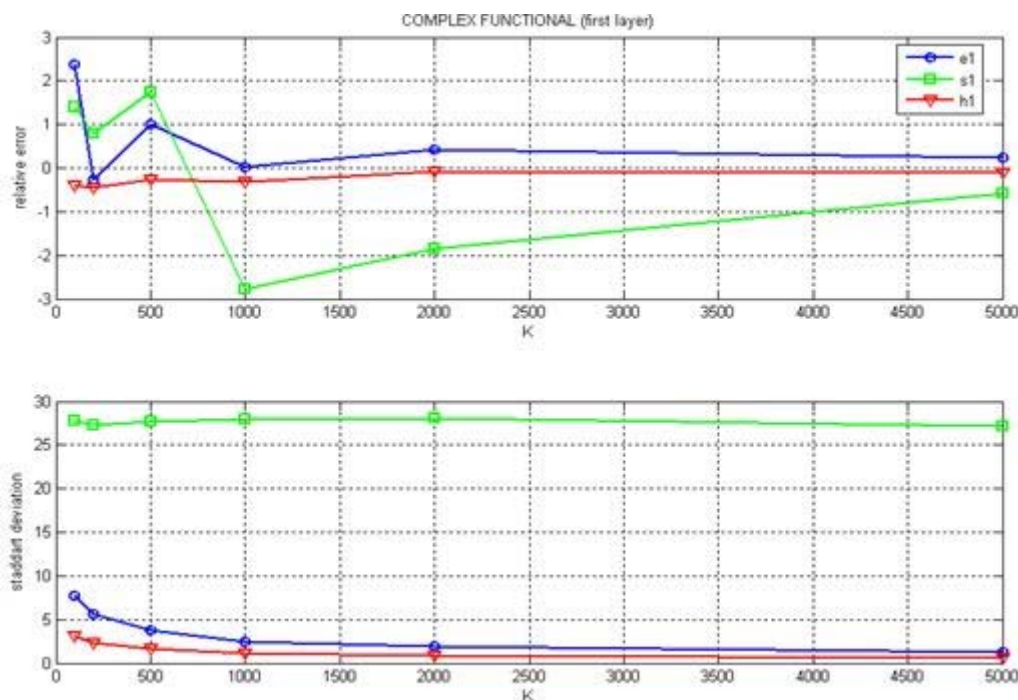


Figure 7. Influence of value  $K$  on accuracy reconstruction of first layer (base) parameters for using aim function  $\Phi_2$

**Influence of value K on second layer (base) parameters reconstruction (Figure 8).** Influence of value K on of relative RMS errors of second layer parameters reconstruction is similar to those of the first layer's. The difference is in higher values of relative RMS errors for  $\varepsilon_2$  and  $h_2$ , as it is shown on Figure 2 and Figure 3. Correspondingly the values of  $\varepsilon_2$  and  $h_2$  are higher although they decrease with the increase of K when using the aim function  $\Phi_1$  (Figure 8,a). When using the aim function  $\Phi_2$   $\varepsilon_2$  and  $h_2$  are less than 1% already when  $K = 1000$  (Figure 8,b). Dependence of  $\sigma_2$  has also a chaotic character as for  $\sigma_2$  RMS error is independent of K (Figure 4).

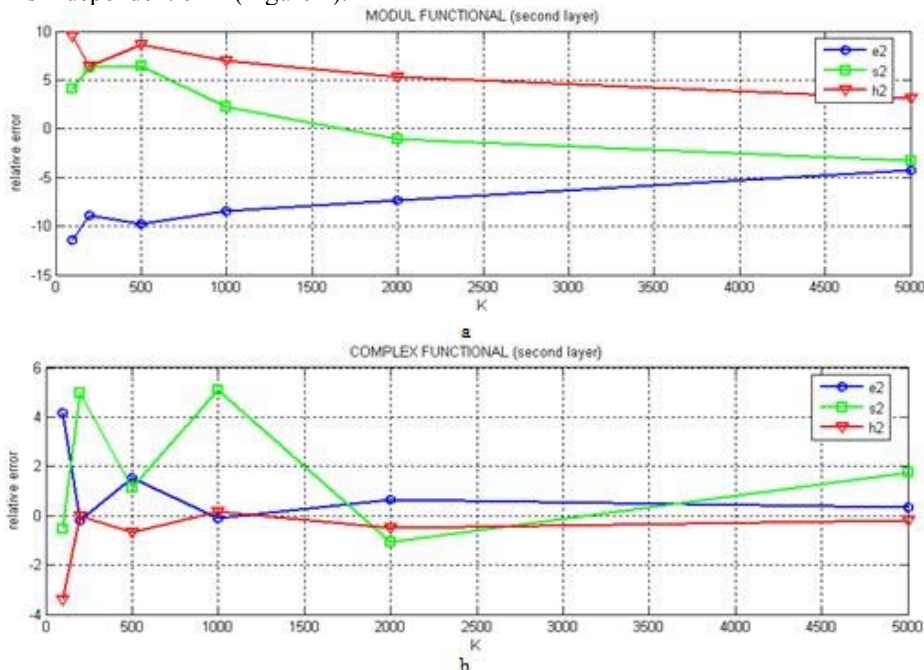


Figure 8. Influence of value K on accuracy reconstruction of second layer (base) parameters for using aim function  $\Phi_1$  (a) and aim function  $\Phi_2$  (b)

**Influence of value K on lower semi-infinite space (subgrade) parameters reconstruction (Figure 9).** Increase of value K leads to decrease of RMS errors for  $\varepsilon_3$  and  $h_3$  and therefore to decrease of relative errors of these parameters reconstruction.

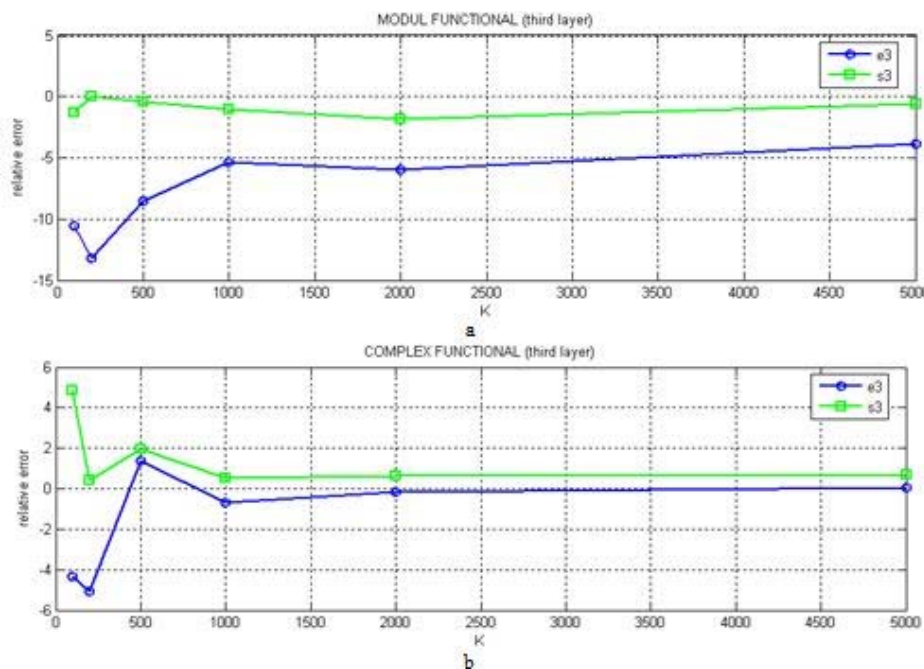


Figure 9. Influence of value K on accuracy reconstruction of lower semi-infinite space (sub grade) parameters for using aim function  $\Phi_1$  (a) and aim function  $\Phi_2$  (b)

When  $K > 1000$  the relative errors hardly change. Using the aim function  $\Phi_2$  allows to obtain  $\varepsilon_3$  and  $h_3$  with relative error less than 1% already when  $K = 1000$  (Figure 9,b).

**3.2. Influence of frequency range on the error of parameter reconstruction of the modelled medium**

Solving of a subsurface radar probing inverse problem in a frequency area can be performed with different number of spectral components, i.e. in frequency ranges of a different width as well as differently positioned on the frequency axe. The aim of choosing of the optimal frequency range is minimizing the relative error determination of medium electro-physical parameters: dielectric permittivity  $\varepsilon$ , electrical conductivity  $\sigma$  and the layer thickness  $h$  for all layers of roadway structure.

In this work solving of the inverse problem was carried out in the frequency range  $[f_1 \dots f_{max}]$ , where  $f_1$  – is the frequency of the first spectral component, equal to 10 MHz, and value of  $f_{max}$  was changing in range from 50 MHz to 500 MHz. Influence of  $f_{max}$  on the solution of the inverse problem was researched with two values of  $K$ :  $K = 1000$  and  $2000$ . Both aim functions  $\Phi_1$  and  $\Phi_2$  were used in our experiments. Analysis of results shows that using aim function  $\Phi_2$  allowed to achieve lower relative error of parameter reconstruction compared to the results obtained using aim function  $\Phi_1$ . Figure 10 illustrates influence of  $f_{max}$  on the relative error of pavement (first layer) and base (second layer) parameters reconstruction when aim function  $\Phi_2$  is used. From this figure one can see:

- relative error of parameter reconstruction  $h_1, \varepsilon'_1$  (Figure 10,a),  $h_2$  and  $\varepsilon'_2$  (Figure 10,b) is less than 1% when  $f_{max} > 100$  MHz and is independent of  $K$ ;
- relative error of parameter reconstruction  $\sigma_1$  and  $\sigma_2$  has a complex dependence on  $f_{max}$ .

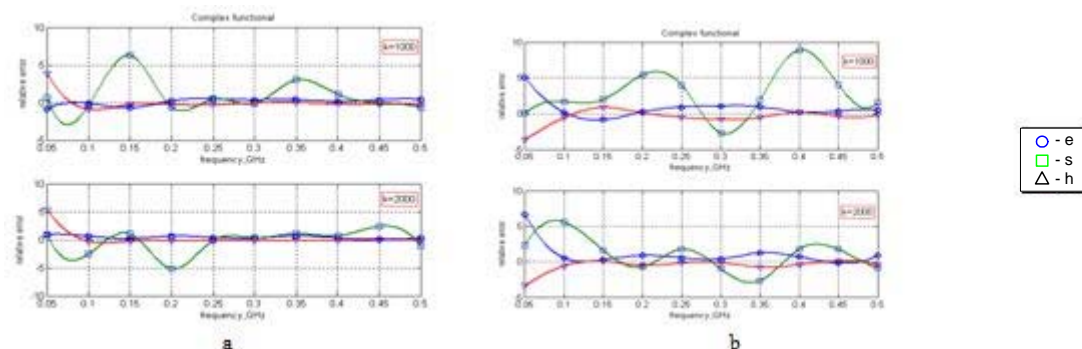


Figure 10. Influence of  $f_{max}$  on the relative error of the first layer parameter reconstruction (a) and the second layer parameter reconstruction (b) using  $\Phi_2$

The similar character of the dependencies shown in the Figure 15 can be explained by the fact that the electro-physical parameters of the first (pavement) and second (base) layers have an identical affect on  $\Phi_2$ , where as an increase of  $f_{max}$  does not change the size of the areas around the global minimum, values of which are less of  $\alpha$  (Figures 2,b and 3,b). When aim function  $\Phi_2$  is using then relative errors of  $\sigma_3$  and  $\varepsilon'_3$  determination are approximately 1%. Note that when  $K = 2000$  the values of the above variables can be obtained when used maximal frequency of reflected signal is in range  $100\text{ MHz} \leq f_{max} \leq 450\text{ MHz}$ .

**3.3. Influence of value K and of GA characteristics on the time for solving of inverse problem**

As an estimate time for solving the inverse problem, we use the average population amount (iterations) of GA (Figure 11). When using the aim function of  $\Phi_2$ , this quantity depends linearly on  $K$ . This means that the inverse problem always ends up as a result of the condition  $\Phi_2 < \alpha$  (2.6). When using the aim function  $\Phi_1$  average population amount virtually unchanged for  $K > 2000$ . Consequently, for such values of  $K$  the solving of inverse problem stops more often if the number of iterations exceeded admitted number of population 500.

We have investigated the influence on the time for solving of inverse problem of the following GA characteristics: population size (number of individuals in the population) and bits of individuals (number of bit per parameter). Investigations conducted for the two aim functions  $\Phi_1$  and with fixed values of  $f_{\max} = 300$  MHz and  $\alpha$  ( $K = 1000$ ). Investigations show that these characteristics of genetic algorithm does not affect on the error of parameter reconstruction of the probed medium parameters. Terms of the end of inverse problem solving the (2.5 and 2.6) exclude the influence of these genetic algorithm characteristics. The population size varied from 20 to 1000 individuals.

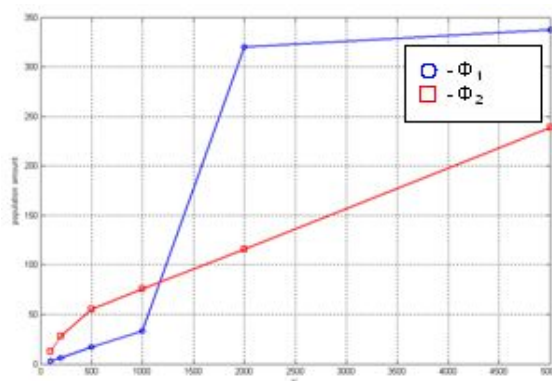


Figure 11. Influence of value K on population amount for using aim functions  $\Phi_1$  and  $\Phi_2$

Changing the number of individuals can change the time for solving of inverse problem. Dependence of the population amount (iterations), which were necessary for solving of the inverse problem, on the population size is shown on Figure 12.

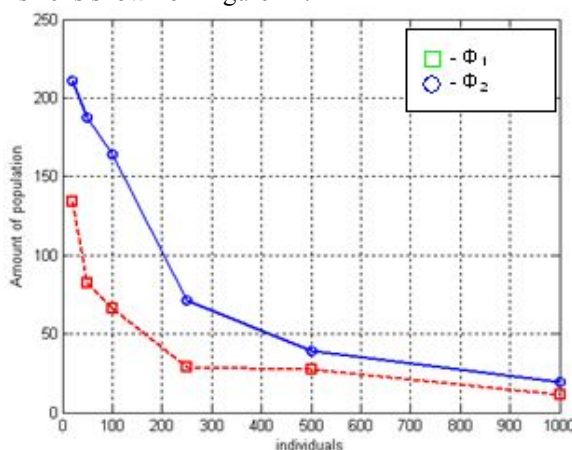


Figure 12. Influence of the population size on population amount for using aim functions  $\Phi_1$  and  $\Phi_2$

If the number of individual increases, it will increase the probability that in the next generation will be an individuals, whose aim functions are less than  $\alpha$ , ie more probability to end the inverse problem in the current population. When aim function  $\Phi_1$  is using then amount of populations required less, although the reconstruction error of electrical parameters of the probed medium are noticeably lose (3.1., 3.2.). If the number of individuals of more than 250, the amount of population does not decrease significantly. This means that the time for solving the inverse problem will increase due to growth in population size. Consequently, the maximum size of an individual should not be more than 200 ... 500.

#### 4. Hardware Implementation of Genetic Algorithm for Solving of the Inverse Problem of Subsurface Probing

##### 4.1. Block diagram of the device for solving the inverse problem with using genetic algorithm

Hardware implementation of the device for solving the inverse problem of subsurface probing will create a portable automated (intelligent) system (device) for radar monitoring of the roadway. If we consider the algorithm shown on Figure 1, from the viewpoint of hardware implementation, we can distinguish two main objectives of hardware implementation:

- hardware implementation of genetic algorithm;
- hardware implementation of computing a aim function (fitness function).

Operators of the classic genetic algorithm are executed sequentially (Figure 13). When the hardware implementation of the genetic algorithm should consider the following features:

- for each individual or pair of individuals can arrange a separate process - parallel processing of all individuals in a population at each stage of the genetic algorithm;
- consistent application of all operators of the GA allows organizing the pipelining of all individuals.

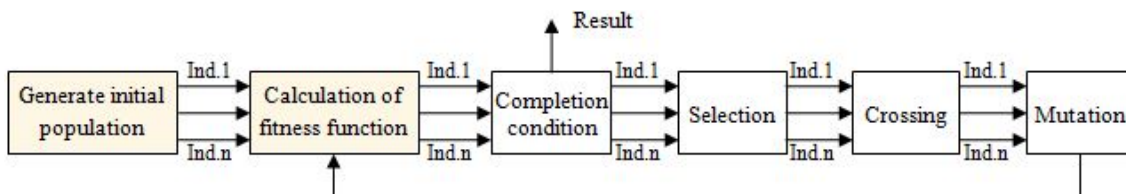


Figure 13. Flowchart of genetic algorithm

Each operator of genetic algorithm is a combination of elementary operators of Boolean algebra and applied to binary vectors. Therefore, micro controllers, digital signal processors or programmable logic arrays can be used for the hardware implementation of genetic algorithm; produced by analysis of the suitability of these devices for the hardware implementation of genetic algorithm. As programmable logic array has been selected programmable logic arrays such as FPGA. Criteria that assess the suitability of the above devices and estimations of suitability are presented in Table 1.

Table 1. Suitability of electronic devices for the hardware implementation of genetic algorithm

Criteria	Microcontroller	Digital Signal Processors	FPGA
Bit	Fixed	Fixed	Arbitrary
Clock frequency	Low	High	Medium
Effect of population size at run-time of genetic algorithm operators	Strong	Medium	Weak
Possibility of calculating the run-time of genetic algorithm operators	Good	Good	No
The possibility of implementing a quick calculation of the values of complex fitness functions	Bad	Medium	Good
The possibility of organizing parallel execution of genetic algorithm operators	No	Weak	Good
The complexity of making changes to the algorithm of the device for parallel execution of the genetic algorithm	-	Strong	No
The opportunity of pipelining for parallel execution of the genetic algorithm	No	No	Has
The complexity of the algorithm changes of the device	Strong	Medium	Weak

An analysis of the suitability assessment suggests that the FPGA is preferred for hardware implementation of genetic algorithm. Using the FPGA allows pipelining for parallel execution of the genetic algorithm and good opportunities for parallel execution of the genetic algorithm and rapid calculation of complex aim function values. The above features offer a maximum speed of the implemented device. Taking into account the architectural features of FPGA, a block diagram of the device for solving the inverse problem with using genetic algorithm was developed, which is shown on Figure 14.

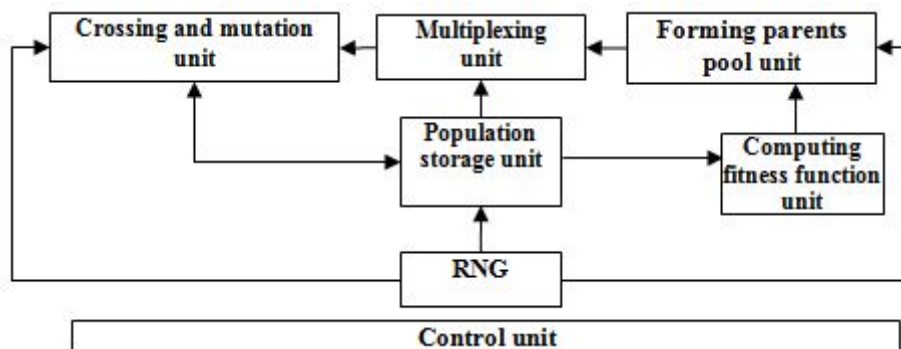


Figure 14. Block diagram of the device for solving the inverse problem with using genetic algorithm

Population storage device represents a block of memory cells. Each memory cell has its input and output ports, allowing for simultaneous treatment of all the memory cells. Each individual is stored in a single memory cell and has its own unique address.

Random number generator (RNG) generates random numbers with uniform distribution law. Random numbers are used to generate individual and addresses of individual, for a random selection of individual, to produce the parent pool, and to ensure the random nature of the operations of mutation and crossover.

Forming parents' pool device serves as a breeding. This device provides a device multiplexing the address of the chromosomes selected in the parent pool. Multiplexing device passes from the memory device of individuals in crossing and mutation device themselves in accordance with their addresses. Crossing and mutation device performs crossover and mutation at the same time, thus saving time and resources to the FPGA. The control unit has links with all the devices of the block diagram and provides the necessary sequence of operations of genetic algorithm and synchronization of all devices circuits.

Some options for hardware implementation in FPGA of some devices were investigated. The investigation purpose is to determine the fastest and least resource-intensive implementation of the genetic algorithm operators. Investigations were conducted by using the software package WebPack ISE, all characteristics were obtained for the family of crystal FPGA Spartan-6.

#### 4.2. Hardware implementation of the forming parents pool device

In terms of hardware implementation is the most profitable tournament selection method. When using the method of selection based on the roulette you need to sum the values of fitness function of individuals. At one level of the logic can be executed only one summation. If the number of parallel processed chromosomes equal to  $2^N$ , then  $N$  must be level logic to calculate the sum of fitness function of chromosomes. It takes a lot of FPGA resources and reduces the speed of device selection. Therefore, the choice of the selection method based on the roulette for hardware implementation of genetic algorithm is potentially disadvantageous.

Tournament selection method is implemented by two devices: comparison unit and the device selection of the individual. The inputs of the device came four values of the fitness function of individuals and their addresses. The output device is given the address of best individuals that participated in the tournament.

The choice of individuals for the tournament can be random or deterministic. In variant of the deterministic selection of individuals the population is divided into groups, including 4 individuals. For each group of tournament selection is carried out. As a result, 25% of individuals of parental pool (upper level) is formed. Another 25% of individuals are selected by dividing the total population into four parts, which are extracted from the chromosome, standing in the same positions in each of the (average level). The remaining 50% of individuals are selected using the following algorithm: choose the first and second individuals  $s$  from the end and the beginning of the population, then the second and third individuals from the beginning and the end of the population, etc. When the deterministic choice of individuals during the formation of the parent pool and a flow of resources will be determined by the FPGA device of the tournament.

For case of a random selection address of individuals is formed by RNG. Figure 15 shows a schematic diagram of the device forming the parent pool for random selection of individuals.

The inputs of each data multiplexer fed fitness function values of all individuals simultaneously. The inputs to select the channel multiplexer receive randomly generated addresses. As a result, the

comparator (CMP) received two values of fitness function and the address of the individuals. The result of comparison is the address of the individual having the highest value of fitness function, which is issued on the external pins device.

For a random selection of chromosomes during the formation of the parent pool and consumption of resources will be determined by the FPGA multiplexers that provide a random selection of individuals.

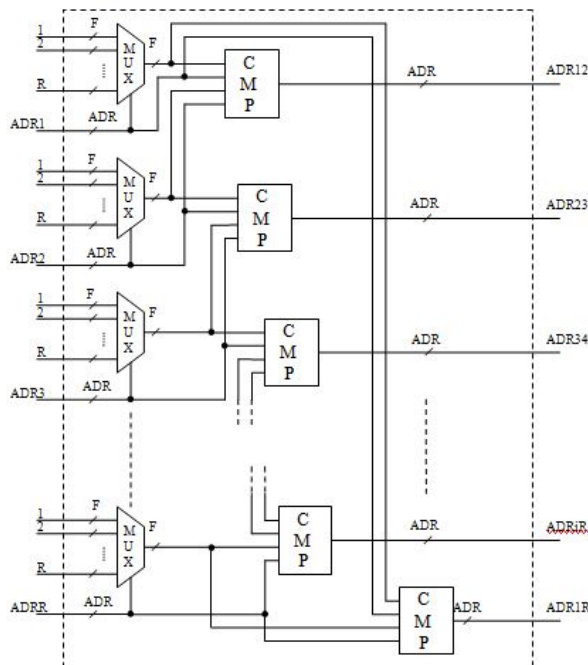


Figure 15. The device forming the parent pool for random selection of individuals

We have investigated the influence of population size:

- on the delay in forming a parent pool device for random selection of individuals (Figure 16, a) and the deterministic choice of chromosomes (Figure 16, b);
- on the use of LUT unit forming the parent pool for random selection of chromosomes (Figure 17,a) and the deterministic choice of chromosomes (Figure 17, b).

There are F - bit of aim function value, and R – the population size in these Figures .It is evident that a more rapid and effective method of choice is a deterministic choice of the individuals for parent pool. However, it is necessary to study the effect of this choice on the convergence of genetic algorithms in general, as the savings in time at this stage may lead to an increase in time to find an inverse problem solution.

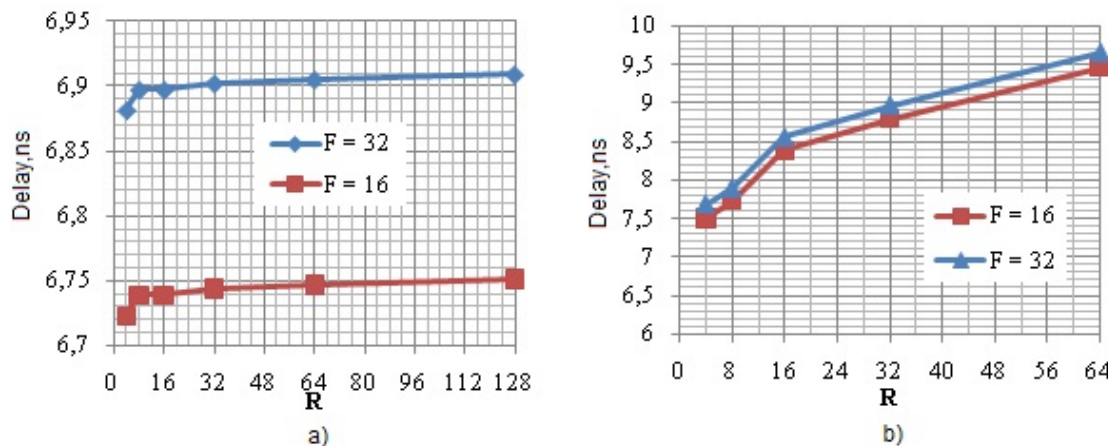


Figure 16. Influence of the population size on the delay in forming a parent pool

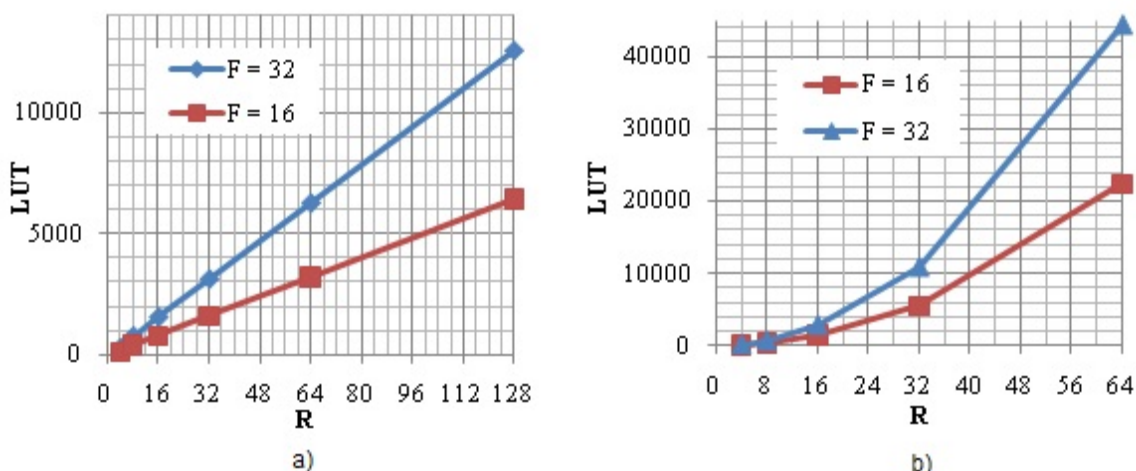


Figure 17. Influence of the population size on the using of LUT unit forming the parent pool

At a random choice the optimal number of parallel processed individuals is 32; for a fixed choice of individuals and at the same cost of resources 128 individuals can be treated. This population size reduces the number of iterations needed to find a solution.

### 4.3. Hardware implementation of the crossing and mutation device

The device must comply with crossing of individuals, selected at the stage of selection. The functional diagram of the device for crossing one pair of individuals is shown on Figure 18. The inputs of the device serve two parental individuals (P1 and P2) and the number of crossing point (T\_C). Comparisons device compare the number of each bit with the number of crossing point, and depending on the result of comparing the multiplexer passes the output bit of one individual or another individual level, thus forming the two individuals are descendants (CH1 and CH2). L – is bit of individuals.

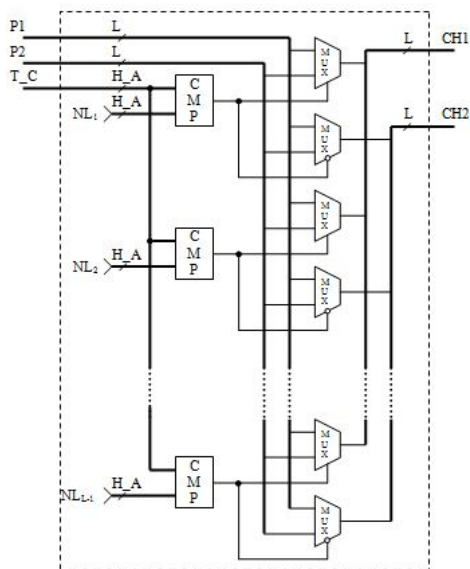


Figure 18. Functional diagram of the crossing device

Figure 19 shows the using of FPGA resources and time delay on the bit of the individuals, respectively.

For a crossing device requires a small amount of FPGA resources. The device has a high speed, it can be used with great individual bit (for example, when a large number of parameters of the aim function) and a large number of parallel processed individuals. The device of mutation is offered combined with a crossing device.

RNG has been implemented on the basis of parallel bit Fibonacci generators. This allowed us to receive one individual in a single cycle of the RNG at a low cost of logical resources. In forming the entire population in one cycle the number of required resources increases in R.

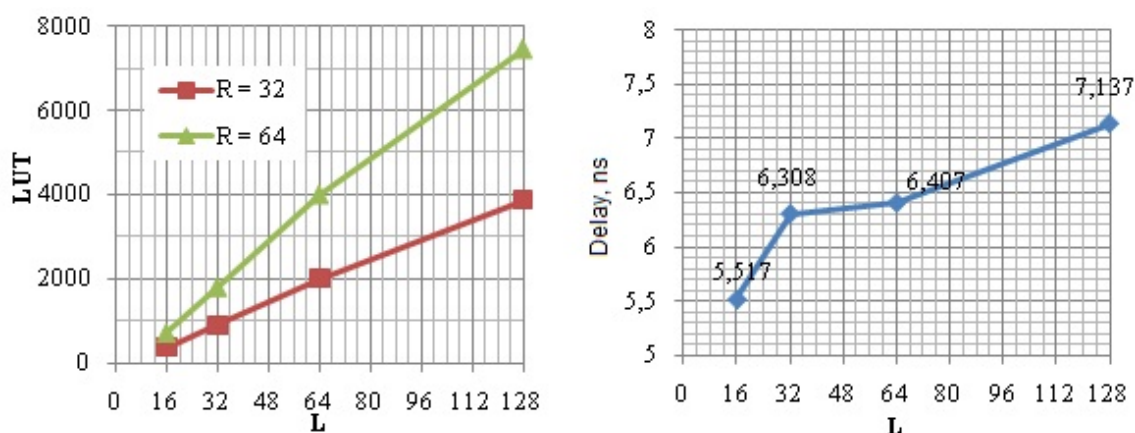


Figure 19. Influence of bits of chromosomes on the using of LUT device crossing (a) and the time of the delay in the crossing device (b) with use multiplexers

## 5. Conclusions

The main results are as follows:

- using complex spectral density  $S(\omega)$  as an informational characteristic increases sensitivity of an aim functions to changes in parameters of the probed medium;
- using an aim function  $\Phi_2$  with a complex spectral density of reflected signal allows for regeneration of  $\varepsilon'$  and  $h$  of the layers with error less than 1%, which is not possible to achieve using an aim function  $\Phi_1$  with a module of spectral density;
- the implementation of selection with a random selection of individuals requires a substantial expenditure of FPGA resources due to the introduction of additional multiplexing devices;
- avoiding the use of random number in the choice of individuals, crossing points etc. to reduce the consumption of FPGA resources, and free resources to spend on increasing the number of parallel processed individuals in order to reduce the search time for solving the inverse problem of subsurface probing.

## References

1. Rexford, M. Morey. *Ground Penetrating Radar for Evaluating Subsurface Conditions for Transportation Facilities (Synthesis of Highway Practice)*. Washington D.C.: National Academy Press, 1998. 37 p.
2. *Ground penetrating radar: theory and applications / Editor Harry M. Jol*. Elsevier Science, 2009. 524 p.
3. Krainyukov, A., Kutev, V. Model-based results of inverse problem solution for radar monitoring of roadway coverage. In: *Proceedings of the International Conference „Modelling of Business, Industrial and Transport Systems“, 7<sup>th</sup>-10<sup>th</sup> May 2008, Riga, Latvia*. Riga: Transport and Telecommunication Institute, 2008, pp. 169-176.
4. Krainyukov, A., Kutev, V., Opolchenov, D. Reconstruction of the roadway coverage parameters from radar subsurface probing data. In: *Proceedings of the 8<sup>th</sup> International Conference “Reliability and Statistics in Transportation and Communication (RelStat’08), 15<sup>th</sup>-18<sup>th</sup> October 2008, Riga, Latvia”*. Riga: Transport and Telecommunication Institute, 2008, pp. 146-154.
5. Krainyukov, A. and D. Opolchenov. Using genetic algorithm for solution of inverse structural problem for radar subsurface probing, *Computer Modelling & New Technologies*, Vol. 14, No 1, 2010, pp.56-63. ISSN 1407-5806.